Pages: 25-34 / Vol.18 / Issue 2 / Summer- Fall 2025

Journal of Aerospace Science and Technology

Journal Homepage: https://jast.ias.ir

Original Research Article

Observability-Guided Autonomous Path Planning for Quadrotor Navigation in GNSS-Denied Environments

Mohammad-Ali Amiri Atashgah[1*], Samaneh Elahian[2], and Bahram Tarvirdizadeh[3]

1, 2. College of Interdisciplinary Science and Technology, University of Tehran, Tehran, Iran

3. College of Interdisciplinary Science and Technology, School of Intelligent Systems Engineering, University of Tehran, Tehran, Iran

ARTICLE INFO

Received: 28 July 2024
Revised: 16 February 2025
Accepted: 25 February 2025
Available online: 12 April 2025

KEYWORDS:

Real-time autonomous path planning

Observability degree

Initialization process

Monte Carlo path planning

Gram matrix

EKF- active SLAM

ABSTRACT

Localization of a quadrotor in an unknown environment without access to Global Navigation Satellite System (GNSS) data, utilizing Simultaneous Localization and Mapping (SLAM), has shown promising results. Integrating SLAM and the Extended Kalman Filter (EKF) provides precise estimations of both the quadrotor's position and the terrestrial landmark locations. This paper reviews the Observability-Based Path Planning (OBPP) and evaluates its performance compared to Monte Carlo Path Planning (MCPP). Furthermore, due to the importance of the initialization process in path planning for pre-planned methods, the performance of OBPP is evaluated for various initial positions. Simulation results demonstrate that the proposed method offers superior accuracy and greater robustness for different initial conditions, validating its effectiveness in diverse scenarios. The robustness and adaptability of this approach make it a valuable contribution to the field of autonomous navigation, especially in environments where GNSS is unavailable.

DOI:
https://doi.org/10.22034/jast.2025.470258.1201

ABBREVIATION

SLAM	Simultaneous Localization and Mapping	EKF	Extended Kalman Filter
OBPP	Observability-Based Path Planning	GNSS	Global Navigation Satellite System
MCPP	Monte Carlo Path Planning	RMSE	Root Mean Square Error

* Corresponding Author's Email: atashgah@ut.ac.ir

Print ISSN:1735-2134 Online ISSN: 2345-3648

1 INTRODCTION

The ability of autonomous navigation in GNSS-denied, unknown environments has been a major focus of extensive research across aerial, terrestrial, and marine robotic systems [1]–[3]. Autonomous movement is essential to various robotic applications, including delivery [4]–[6], pesticide dispersion on farms [7], aerial photography of specific locations, and pipeline inspection [7]–[9]. Path planning algorithms are employed with specific criteria to determine the optimal navigation path in each of these applications.

Some path planning methods are based on Graph search algorithms, which are utilized to define the shortest path regarding a specified cost function, such as A* and D path planning [10]–[12]. Other methods, such as the probabilistic roadmap method (PRM) and Rapidly-exploring Random Tree (RRT), are based on sampling and focus on optimizing the speed of path planning [13]–[17]. Barrier collision avoidance-based methods, such as cell decomposition and potential field (PF) approaches [11], [18], [19], as well as optimization-based methods [20], determine the path by considering environment barriers. Another category includes methods that dynamically define the movement path based on real-time sensor information. Carlone proposed a method in which the path is continuously adjusted using information gathered from the robot's sensors, allowing it to navigate effectively toward its destination [21]. Kalogeiton and Sharma introduced an adaptive cognitive-based optimization algorithm for path planning and evaluated its effectiveness against random methods [22], [23]. In the random path planning method, the following point for the robot motion is selected stochastically from the limited space of the points ahead of the robot. Bryson raised entropy criteria to measure the environmental information at each step [24]. In their research, entropy is introduced to measure the compactness of the landmarks distribution and thus measure their information. So that, more entropy results in less information. Leung planned the path to maximize the specified area coverage [25].

This paper reviews the concept of observability degree in the context of real-time path planning for a quadrotor in unknown environments, focusing on the OBPP. System observability refers to the ability of a system to estimate its inputs accurately by measuring the outputs. A conventional approach to determine the system's observability is the Hermann and Krener method, which involves evaluating the rank of the observability matrix [26]. While in some applications, it is crucial to quantify the observability of a system. Various matrices and criteria have been proposed to define the degree of observability in nonlinear systems. Liang et. al. discussed three main categories based on: covariance, observability, and information matrices [27]. Matrices such as Lie derivative, observability, covariance, and Gramian are commonly used to obtain the degree of observability. The Lie derivative matrix is used primarily to determine whether the system is observable and to what extent. In contrast, the covariance, observability, and Gramian matrices provide a more precise evaluation considering parameters such as determinant, trace, eigenvalues, and singular values. A summary of the matrices and related parameters used to determine the observability degree is presented in Table 1, as outlined in the literature.

Table 1. Different methods for observability degree analysis in the literature

matrix	Parameter	Reference
covariance	Trace	[28]
	Eigenvalue	[29]
	Determinant	[30]
Gramian	trace, near singularity, condition number	[31]
	trace, eigenvalue	[32]
	Determinant	[33]
observability	SVD	[34], [35]
Lie	observability rank, to define the observable and unobservable modes	[36]–[38]

This paper aims to evaluate the accuracy of the OBPP [39] by comparing it with the MCPP [40]–[42] for active simultaneous localization and landmarks mapping in an unknown environment. The RMSE between the true and estimated path is utilized as the evaluation criterion for this comparison. To fulfill the proposed path planning method, the maximum eigenvalue and its corresponding eigenvector of the Gram matrix are used to determine the system's observability degree. Sections Ⅱ and Ⅲ present the EKF-SLAM equations and the concurrent path planning within SLAM, referred to as active SLAM. Following this, the MATLAB simulation results for the OBPP are discussed and compared with the MCPP. In the MCPP, each step of the quadrotor's motion is defined randomly from the points in the

allowed points toward the target points. The path to the target that does not have a sufficient number of landmarks at each step is eliminated, and an alternative path is replaced.

2. METHODS

2.1. EKF-SLAM

SLAM is introduced as a solution for robot motion in unknown, GNSS-denied environments, enabling both localizing the robot and mapping the landmarks in the environment. The implementation of EKF-SLAM has shown promising performance [43]–[45]. The estimation equations are derived based on the state and covariance matrices, which are outlined as follows:

$$X = \begin{bmatrix} x_r & y_r & z_r & u & v & w & \varphi & \theta & \psi \\ x_{l1} & y_{l1} & z_{l1} & \cdots & x_{lm} & y_{lm} & z_{lm} & & \end{bmatrix}^T \quad (1)$$

$$P_k = \begin{bmatrix} P_{RR} & P_{Rl} \\ P_{Rl} & P_{ll} \end{bmatrix}_k \quad (2)$$

The state matrix includes data for both the quadrotor and landmarks (Figure 1). The quadrotor data consists of position (x_r, y_r, z_r), linear velocity (u, v, w) aligned with the coordinate axes, and Euler angles (φ, θ, ψ). The position of the i^{th} landmark, represented by x_{li}, y_{li} and z_{li} in the navigation frame, is appended to the end of the state vector.

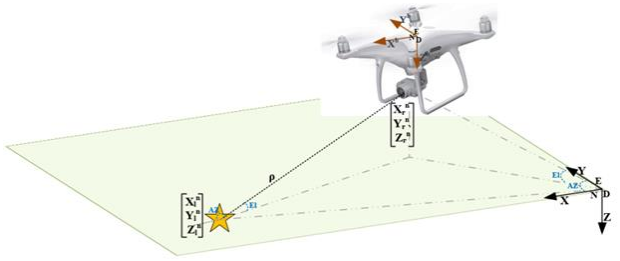

Fig. 1. Quadrotor position and attitude in the NED coordinate system

The covariance matrix quantifies the uncertainty in state parameters and the cross-correlation terms between the quadrotor and landmarks within its field of view (FOV). The state and covariance matrices are predicted and updated using process and observation models. Prediction equations are as follows:

$$X_k^- = f\left(X_{k-1}^+ . u(k)\right) + w(k) \quad (3)$$

$$P_k^- = F_{x.k} P_{k-1}^+ F f_{x.k}^T + F_{w.k} Q_{k-1} F_{w.k} \quad (4)$$

Where $F\_(x.k)=\partial f/(\partial X\_R)$ and $F\_(x.k)=\partial f/\partial w$ represent the Jacobians of the process vector with respect to the robot state and noise vectors, respectively. Meanwhile, w and Q denote Gaussian process noise and its covariance. The update of the covariance and state matrices is calculated using the following equation:

$$\hat{X}_k^+ = \hat{X}_k^- + K_k\{Z_k - h(\hat{X}_k^-)\} \quad (5)$$

$$P_k^+ = (I - K_k H_k) P_k^- \quad (6)$$

Where $H = \frac{\partial h}{\partial X_R}|_{R_k^-, l_k^-}$ is the Jacobian of the observation model. In these equations, S and K denote covariance residual and Kalman gain, respectively, calculated by Eq. 7 and Eq. 8:

$$\hat{X}_k^+ = \hat{X}_k^- + K_k\{Z_k - h(\hat{X}_k^-)\} \quad (7)$$

$$P_k^+ = (I - K_k H_k) P_k^- \quad (8)$$

The process and observation models are defined by Eq. 9 and Eq. 10, Where $\delta_x = x_{lj} - x_{ri}$,$\delta_y = y_{lj} - y_{ri}$ and $\delta_z = z_{lj} - z_{ri}$ represent the position differences between the quadrotor and landmarks in the navigation frame.

$$f = \begin{bmatrix} \Delta P^n(k+1) \\ \Delta V^n(k+1) \\ \Delta \psi^n(k+1) \end{bmatrix} = \begin{bmatrix} v^n(k)\Delta t \\ [C_b^n(k)a^b(k) + g^n]\Delta t \\ E_b^n(k)w^b(k)\Delta t \end{bmatrix} \quad (9)$$

$$h = \begin{bmatrix} \rho_{RL} \\ az \\ el \end{bmatrix} = \begin{bmatrix} \sqrt{(\delta_x{}^2 + \delta_y{}^2 + \delta_z{}^2)} \\ tan^{-1}(\frac{\delta_y}{\delta_x}) \\ tan^{-1}(\frac{\delta_z}{d_{RL}}) \end{bmatrix} \quad (10)$$

The superscripts n and b denote navigation and body frame parameters, respectively. The parameters a^b, g^n, and w^b represent the linear acceleration measured in the body frame, the gravitational vector in North-East-Down (NED) frame, and the angular rates in the body frame, respectively. C_b^n and E_b^n are the transformation and rotation matrices that map coordinates from the body frame to the navigation frame.

$$C_b^n = \begin{bmatrix} C_\psi C_\theta & -S_\psi C_\varphi + C_\psi S_\theta S_\varphi & S_\psi S_\varphi + C_\psi S_\theta C_\varphi \\ S_\psi C_\theta & C_\psi C_\varphi + S_\psi S_\theta S_\varphi & -C_\psi S_\varphi + S_\psi S_\theta C_\varphi \\ -S_\theta & S_\varphi C_\theta & C_\varphi C_\theta \end{bmatrix} \quad (11)$$

$$E_b^n = \begin{bmatrix} 1 & S_\varphi t_\theta & C_\varphi t_\theta \\ 0 & C_\varphi & -s_\varphi \\ 0 & S_\varphi sec_\theta & c_\varphi sec_\theta \end{bmatrix} \quad (12)$$

In SLAM, the covariance and state matrices are dynamic. When the robot moves and detects landmarks within its field of view (FOV), the relevant data is added to the state and covariance matrices before the prediction step. If the landmarks remain within the FOV, the data is updated; if the landmarks go out of the robot's FOV, the corresponding data is removed from both matrices. In the following, the proposed path planning method is described.

2.2. Observability-Based Path Planning

To provide a better comparison between the path planning methods, this section presents a brief review of the OBPP approach. Overall, three main blocks are defined for robot motion: guidance, control, and navigation. Within the control block, a controller generates the necessary commands to adjust the quadrotor's position and attitude, guiding it toward the destination values calculated in the guidance block. In the navigation block, the current attitude is measured, and the position of the quadrotor is calculated. This paper primarily focuses on comparing two path planning methods, OBPP and MCPP, employed within the guidance block. This block determines the quadrotor's desired position through the path planning algorithm. Both methods are suitable for GNSS-denied environments. The OBPP is an autonomous online path planning method that determines the path of robot motion with respect to the terrestrial landmarks in each step, while the MCPP is a pre-programmed method that requires prior information about the environment.

2.2.1. Degree of Observability

Various methods have been proposed in the literature to measure the observability of nonlinear systems [34], [46]–[49]. When a system is observable, it indicates that the system's inputs can be estimated more accurately from the measured outputs [50]–[52]. However, these methods do not provide a direct measure of the degree of observability of the system. The concept of observability degree quantifies the extent to which a system is observable. Accordingly, defining a matrix and specific criteria for measuring the observability is necessary. In this context, the Gramian matrix and its eigenvalue are selected as a matrix and a criterion for the observability measurement. The degree and direction of observability are determined by the eigenvalue and its associated eigenvector, respectively. For a nonlinear system, the Gramian is calculated by defining the transition and output matrices and linearizing the nonlinear system using Taylor expansion (Eq. 13) and Lyapunov equation (Eq. 14) [52].

$$\begin{aligned} X_{k+1} &= A_d X_k + B_d u_k \\ Z_{k+1} &= C_d X_k + D_d u_k \end{aligned} \tag{13}$$

$$\mathrm{A^T W_o} + \mathrm{W_o} A + C^T C = 0 \tag{14}$$

The solution to the Lyapunov equation is determined using Eq. 15.

$$\mathrm{W_o(t)} = \int_0^{\mathrm{t}} \mathrm{e^{A^T \tau} C^T C e^{A\tau} d\tau} \tag{15}$$

Calculating the exact value of the Gramian using the above equations for high-dimensional systems is complex, computationally expensive, and impractical [53]. A more efficient and approximate calculation of the Gramian is computed by Eq. 16.

$$\mathrm{W_o} \approx \mathrm{O_d^T O_d} \tag{16}$$

$\mathrm{O_d}$ is a discrete-time observability matrix.

$$\mathrm{O_d} = \begin{bmatrix} \mathrm{C_d} \\ \mathrm{C_d A_d} \\ \mathrm{C_d A_d^2} \\ \vdots \\ \mathrm{C_d A_d^{n-1}} \end{bmatrix} \tag{17}$$

Once the Gram matrix is determined, the degree of observability for various linear combinations of state vector parameters can be defined. This process involves calculating the Gramian matrix for the n landmarks at time t within the quadrotor's field of view (FOV), followed by the computation of its eigenvalues and eigenvectors. The eigenvector corresponding to the maximum eigenvalue indicates the most observable direction for the robot's movement (as shown in Eqs. 18 and 19). Therefore, it determines the next point for the quadrotor's motion.

$$\lambda_{timax} = \max\left(\lambda_{ti1}. \ldots . \lambda_{tin}\right) \tag{18}$$

$$v_{timax} = \begin{bmatrix} v_{max,x} \\ v_{max,y} \end{bmatrix} \tag{19}$$

To calculate the Gramian as per Eq. 17, the initial position of the quadrotor is put into the active SLAM algorithm, as outlined in Table 2. The corresponding matrices are derived using the specified equation (Eq. 16). Finally, based on the calculated Gramian matrix, the direction of motion for the quadrotor is determined according to the algorithm (Table 2).

Table 2. Active SLAM algorithm with OBPP

Algorithm 1: Algorithm of the active SLAM with OBPP

Mission Starts

EKF- active SLAM **Starts**

Path-Planning Starts

Make an Observability dataset.

For i=1:numLmk **do**

Calculate the observability matrix (O) according to Eq. 13.

Calculate observability Gramian (W_o) by Eq. 18

Determine max eigenvalue of W_0

End

Search the most observable direction.

Find the maximum eigenvalue of all eigenvalues in each step.

Select the eigenvector of the maximum eigenvalue.

$\theta_{rot} = \theta_{MOD} - \theta_{rob}$ (MOD: most observable direction)

Perform Remaining EKF- active SLAM **Tasks**

Path-Planning Ends

EKF- active SLAM **Ends**

Mission Decision-Making Tasks

Mission Ends

3. SIMULATION SCENARIOS AND RESULTS

The proposed path planning method is evaluated by simulating a quadrotor equipped with an IMU operating at a frequency of 200 Hz and external sensors with a sampling rate of 2 samples per second (as shown in Table 3).

Table 3. The quadrotor's internal and external sensor specifications.

IMU		Vision camera specification	
Sampling rate	200 Hz	Sampling rate	2 Hz
Acc noise	0.12 m/s^2	Max. view range	55 m
Gyro Noise	0.28 deg/s	FOV	$60^{ver} \times 180^{hor}$deg

The external sensors measure the distance and bearing to landmarks, which are represented by terrestrial trees randomly placed within the simulation environment. The concept of scenario, the robot's initial point, end zone, and physical realization of the landmarks are depicted in Figure 2.

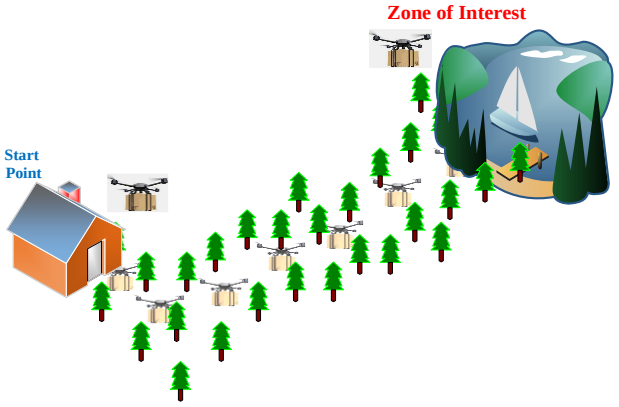

Fig. 2. A virtual designed mission for the quadrotor motion from the start point to the end.

Acceleration and angular rates are measured by internal accelerometer and gyroscope sensors to establish the true path. Using the estimated attitude and current position, the next position is calculated with simplified 6-Degree of Freedom (DOF) equations of the quadrotor. The SLAM path of the quadrotor is defined by the EKF-SLAM algorithm, which incorporates robot observations from external sensors, attitude measurements from internal sensors, and Dead Reckoning (DR) equations. In both methods, the next step of motion is determined by the OBPP algorithm, whereas in MCPP, the next step is defined randomly. To enhance estimation accuracy in MCPP, random paths through areas with a low number of landmarks are discarded.

The trace of the covariance matrix reflects the uncertainty of estimation (Eq. 20).

$$trace(A) = \sum_{i=1}^{n} a_{ii} \quad (20)$$

A smaller trace of the covariance matrix indicates higher estimation accuracy and can serve as a criterion for evaluating precision [54], [55]. Therefore, the trace values and RMSE are compared to provide a complementary understanding of the estimation accuracy in the simulations.

Each terrestrial landmark, represented by a '+' symbol in simulations (like in figures 3 and 4), corresponds to a tree with distinctive features that are extracted using feature extraction algorithms. In simulations, it is assumed that these features are accurately extracted, enabling the quadrotor to identify the landmarks reliably. In other words, the features are known for the quadrotor, and no extraction algorithm is used in simulations.

3.1. Results and Discussion

MATLAB simulations are performed in an arbitrary scenario to compare the performance of OBPP and MCPP methods. In simulations, the robot's path, which is obtained by the robot's equation of motion without considering any noise for the sensors, is called the true path, and the one that is obtained by EKF estimation for noisy sensors in the real environment is called the estimated path. The true path is considered as a reference for evaluating the estimated path in the real implementation of the proposed algorithm's accuracy. These paths obtained by both path planning methods are illustrated in Figures 3 and 4. Moreover, Figures 5 to 8 illustrate the discrepancies between the quadrotor's true and estimated positions in the x, y, and z directions and its roll and pitch attitudes.

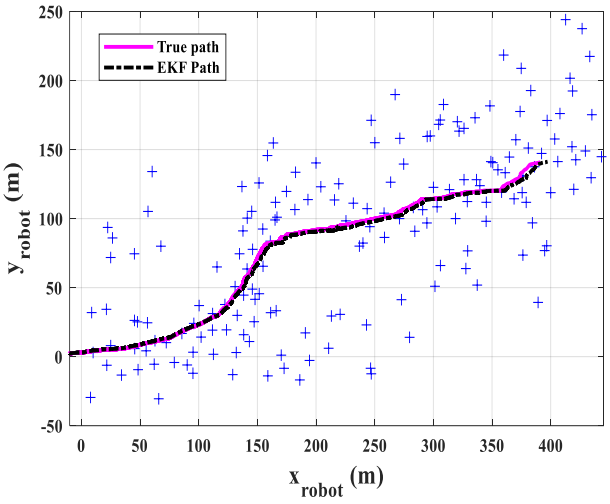

Fig. 3. The quadrotor movement path using OBPP

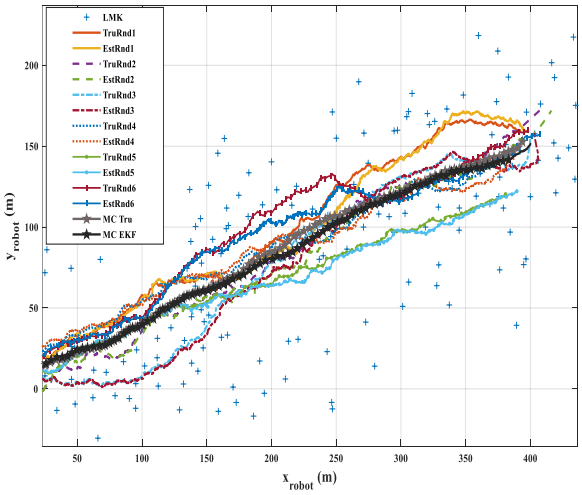

Fig. 4. The quadrotor movement path using MCPP

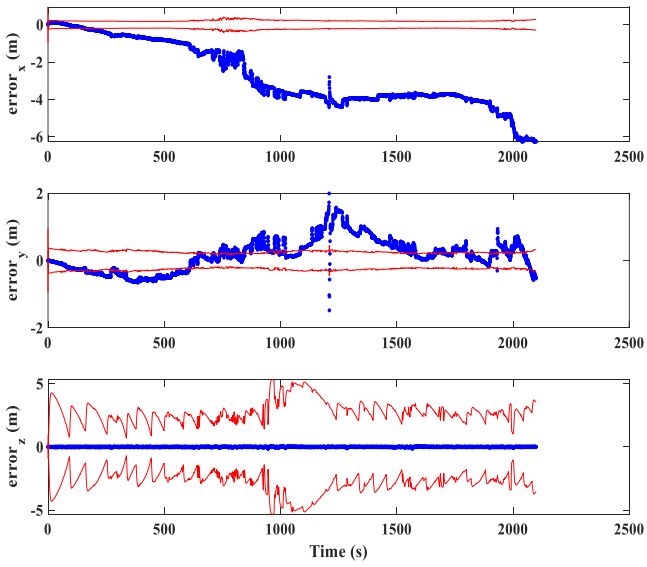

Fig. 5. The quadrotor position error using OBPP and 3σ bounds

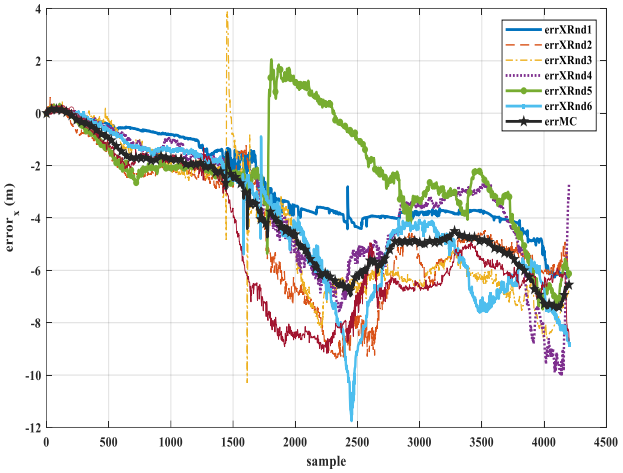

Fig. 6. The quadrotor x-position error using MCPP

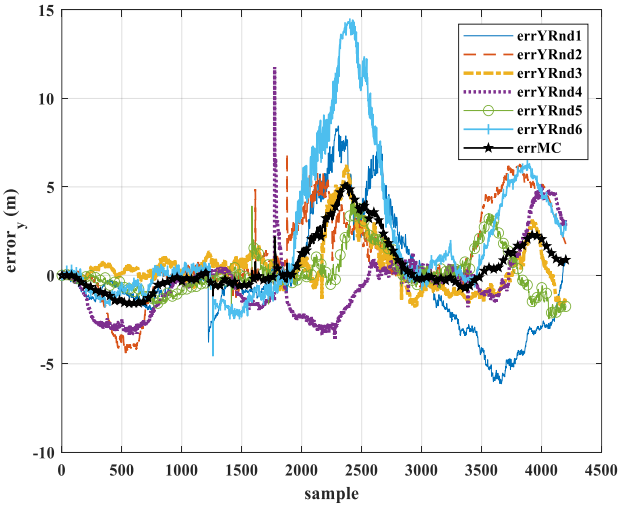

Fig. 7. The quadrotor y-position error using MCPP

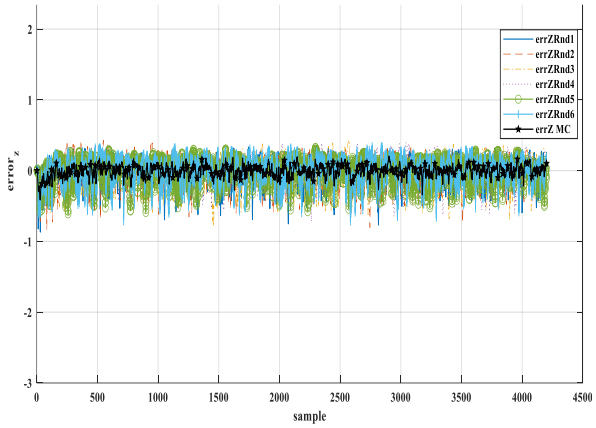

Fig. 8. The quadrotor z-position error using MCPP

The results indicate that the OBPP method enables the quadrotor to autonomously plan a path from the initial to the endpoint without requiring any prior information about the environment or GNSS signals. A comparison between OBPP and MCPP demonstrates that OBPP provides better accuracy in position estimation. Specifically, the RMSE for position estimation is reduced by 27%, 70%, and 79% in the x, y, and z coordinates, respectively. Furthermore, the RMSE for attitude estimation is reduced by 12%. Additionally, the OBPP method achieves a 27% reduction in uncertainty, as indicated by the covariance trace (Table 4).

Table 4. Position and attitude RMSE comparison between the MCPP and OBPP

Path Planning Method	Pos. RMSE total	Att. RMSE total	x RMSE	y RMSE	z RMSE	Trace of Cov.
OBPP	3.2748	0.1219	3.2363	0.4999	0.0172	4720
MCPP	4.7142	0.1387	4.4165	1.6480	0.0828	6490

Initialization plays an important role in quadrotor motion. In methods where the robot's trajectory is predefined, any variation in the initial position can cause the robot to follow an incorrect path, potentially resulting in the inability to observe enough landmarks for effective SLAM execution. A sensitivity analysis was performed to evaluate the impact of initial position variations on the OBPP method. The results highlight the robustness of the OBPP method to changes in the initial position, as shown in Figure 9. Position errors between the true and estimated path determined with the OBPP algorithm and MCPP in the x and y directions are depicted in Figure 10 and Figure 11, respectively.

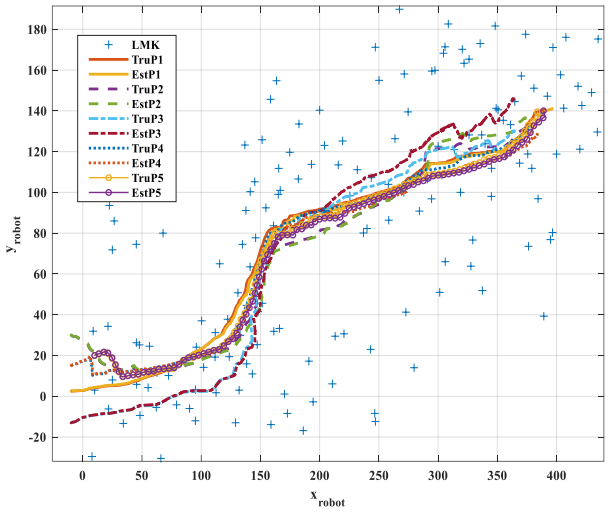

Fig. 9. Quadrotor movement path using OBPP for different initialization

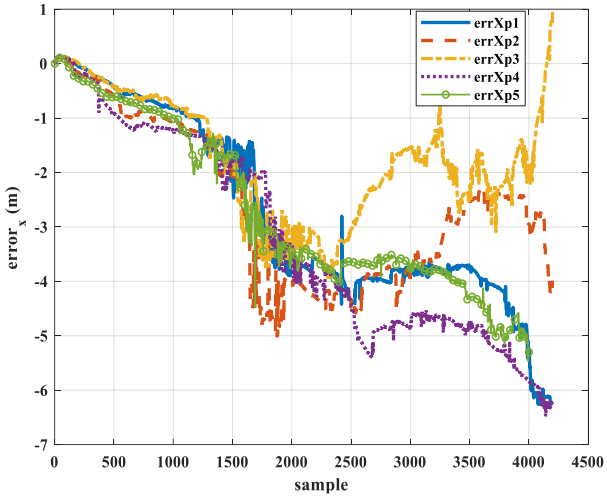

Fig. 10. Quadrotor positioning error in the x-direction using OBPP for different initialization

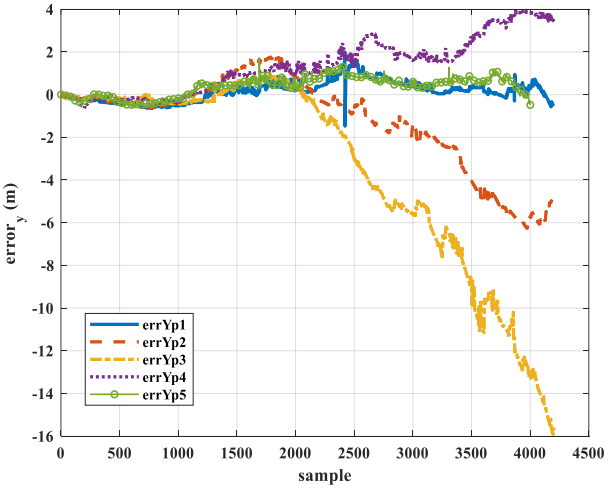

Fig. 1 11. Quadrotor positioning error in y-direction using OBPP for different initialization

Table 5 presents the position and attitude estimation RMSE as the initial point varies. The comparison indicates that the initial point has minimal effect on path planning using the OBPP. The initial point determines the landmarks that are in the robot's FOV. Therefore, the effects of the next point of the robot motion result in different paths for different initial positions.

Table 5. Position and attitude RMSE for different initial positions

	initial point	position RMSE	attitude RMSE
point1	(-10,2.5)	3.2758	0.1219
point2	(-10,30)	3.8408	0.1283
point3	(-10,-13)	6.0595	0.1470
point4	(-10,15)	4.1518	0.1204
point5	(10,20)	3.1385	0.1195

4. CONCLUSIONS

This paper investigates robot motion in a GNSS-denied, unknown environment using EKF-SLAM. The trajectory of a quadrotor in such an environment affects the number of in-range landmarks and, consequently, the state and covariance matrices. These factors ultimately determine the accuracy of state estimation according to the determined path.

To achieve more accurate estimations of the robot and landmarks' positions, OBPP is proposed as an active SLAM approach. This method is developed based on the concept of observability degree. Its accuracy is evaluated by comparing it to the MCPP method. Simulation results indicate that OBPP achieves lower estimation errors compared to MCPP. Another important parameter for path planning techniques, such as Monte Carlo-based methods, is the deviation from the predefined initial position. Initialization errors may cause the quadrotor to follow paths with insufficient landmark coverage, potentially resulting in SLAM failure. However, the OBPP method demonstrates robust path planning capabilities while effectively compensating for the variations in initial position.

CONFLICT OF INTEREST

The authors declare that they have no conflict of interest.

REFERENCES

[1] N. Crasta, D. Moreno-Salinas, A. M. Pascoal, and J. Aranda, "Multiple autonomous surface vehicle motion planning for cooperative range-based underwater target localization," *Annu. Rev. Control*, vol. 46, pp. 326–342, Jan. 2018, https://doi.org/10.1016/j.arcontrol.2018.10.004.

[2] O. M. Cliff, R. Fitch, S. Sukkarieh, D. L. Saunders, and R. Heinsohn, "Online localization of radio-tagged wildlife with an autonomous aerial robot system," *Robot. Sci. Syst.*, vol. 11, Jan. 2015, https://doi.org/10.15607/RSS.2015.XI.042

[3] S. Park and S. Hashimoto, "Autonomous mobile robot navigation using passive RFID in an indoor environment," *IEEE Trans. Ind. Electron.*, vol. 56, no. 7, pp. 2366–2373, 2009, https://doi.org/10.1109/TIE.2009.2013690.

[4] N. Goyal, R. Aryan, N. Sharma, and V. Chhabra, "Line Follower Cargo-Bot for Warehouse Automation," *Int. Res. J. Eng. Technol.*, Vol. 8 issue 2, 2021, [Online]. Available: https://www.irjet.net/archives/V8/i2/IRJET-V8I2179.pdf.

[5] T. Machado, T. Malheiro, S. Monteiro, W. Erlhagen, and E. Bicho, "Multi-constrained joint transportation tasks by teams of autonomous mobile robots using a dynamical systems approach," *Proc. - IEEE Int. Conf. Robot. Autom.*, pp. 3111–3117, 2016, https://doi.org/10.1109/icra.2016.7487477

[6] J. Fayyad, M. A. Jaradat, D. Gruyer, and H. Najjaran, "Deep learning sensor fusion for autonomous vehicle perception and localization: A review," *Sensors (Switzerland)*, vol. 20, no. 15, pp. 1–34, 2020, https://doi.org/10.3390/s20154220.

[7] K. D. Sowjanya, R. Sindhu, M. Parijatham, K. Srikanth, and P. Bhargav, "Multipurpose autonomous agricultural robot," *Proc. Int. Conf. Electron. Commun. Aerosp. Technol. ICECA 2017*, pp. 696–699, 2017, https://doi.org/ 10.1109/ICECA.2017.8212756.

[8] M. Polic, A. Ivanovic, B. Maric, B. Arbanas, J. Tabak, and M. Orsag, "Structured Ecological Cultivation with Autonomous Robots in Indoor Agriculture," *Proc. 16th Int. Conf. Telecommun. ConTEL 2021*, pp. 189–195, Jun. 2021, https://doi.org/10.23919/CONTEL52528.2021.9495963.

[9] H. Durmus, E. O. Gunes, M. Kirci, and B. B. Ustundag, "The design of general-purpose autonomous agricultural mobile-robot: 'AGROBOT,'" *2015 4th Int. Conf. Agro-Geoinformatics, Agro-Geoinformatics 2015*, pp. 49–53, https://doi.org/10.1109/Agro-Geoinformatics.2015.7248088 .

[10] B. Fu et al., "An improved A* algorithm for the industrial robot path planning with high success rate and short length," *Rob. Auton. Syst.*, vol. 106, pp. 26–37, Aug. 2018, https://doi.org/10.1016/j.robot.2018.04.007.

[11] Y. Hasegawa and Y. Fujimoto, "Experimental verification of path planning with SLAM," *IEEJ J. Ind. Appl.*, vol. 5, no. 3, pp. 253–260, 2016, https://doi.org/10.1541/ieejjia.5.253.

[12] Z. Wang and J. Cai, "Probabilistic roadmap method for path-planning in radioactive environment of nuclear facilities," *Prog. Nucl. Energy*, vol. 109, pp. 113–120, 2018, https://doi.org/10.1016/j.pnucene.2018.08.006.

[13] K. Wei and B. Ren, "A method on dynamic path planning for robotic manipulator autonomous obstacle avoidance based on an improved RRT algorithm," *Sensors (Switzerland)*, vol. 18, no. 2, p. 571, Feb. 2018, https://doi.org/10.3390/s18020571.

[14] A. Gasparetto, P. Boscariol, A. Lanzutti, and R. Vidoni, "Path planning and trajectory planning algorithms: A general overview," *Mech. Mach. Sci.*,

vol. 29, pp. 3–27, 2015, https://doi.org/10.1007/978-3-319-14705-5_1.

[15] Y. Li, W. Wei, Y. Gao, D. Wang, and Z. Fan, "PQ-RRT*: An improved path planning algorithm for mobile robots," *Expert Syst. Appl.*, vol. 152, p. 113425, Aug. 2020, https://doi.org/10.1016/j.eswa.2020.113425

[16] S. Karaman and E. Frazzoli, "Sampling-based algorithms for optimal motion planning," *Int. J. Rob. Res.*, vol. 30, no. 7, pp. 846–894, Jun. 2011, https://doi.org/10.1177/0278364911406761.

[17] O. Arslan and P. Tsiotras, "Use of relaxation methods in sampling-based algorithms for optimal motion planning," *2013 IEEE International Conference on Robotics and Automation* 2013. https://di.org/10.1109/ICRA.2013.6630906.

[18] Y. Rasekhipour, A. Khajepour, S. K. Chen, and B. Litkouhi, "A Potential Field-Based Model Predictive Path-Planning Controller for Autonomous Road Vehicles," *IEEE Trans. Intell. Transp. Syst.*, vol. 18, no. 5, pp. 1255–1267, May 2017, https://doi.org/10.1109/TITS.2016.2604240.

[19] Y. B. Chen, G. C. Luo, Y. S. Mei, J. Q. Yu, and X. L. Su, "UAV path planning using artificial potential field method updated by optimal control theory," *Int. J. Syst. Sci.*, vol. 47, no. 6, pp. 1407–1420, Apr. 2016, https://doi.org/10.1080/00207721.2014.929191.

[20] H. Kiaee and H.Reza Heidari, "Cooperative path planning for leader – follower formation of Multi UAV based on the minimum energy consumption for load transportation," *Amirkabir Journal of Mechanical Engineering*, vol. 52, issue 12, 2021, pp. 3327-3340, (in Prsian) https://doi.rg/10.22060/mej.2019.15994.6245.

[21] L. Carlone, J. Du, M. Kaouk Ng, B. Bona, and M. Indri, "Active SLAM and exploration with particle filters using Kullback-Leibler divergence," *J. Intell. Robot. Syst. Theory Appl.*, vol. 75, no. 2, pp. 291–311, Oct. 2014, https://doi.org/10.1007/s10846-013-9981-9

[22] V. S. Kalogeiton, K. Ioannidis, G. C. Sirakoulis, and E. B. Kosmatopoulos, "Real-Time Active SLAM and Obstacle Avoidance for an Autonomous Robot Based on Stereo Vision," *Cybern. Syst.*, vol. 50, no. 3, pp. 239–260, Apr. 2019, https://doi.org/10.1080/01969722.2018.1541599

[23] R. Sharma, R. W. Beard, C. N. Taylor, and S. Quebe, "Graph-based observability analysis of bearing-only cooperative localization," *IEEE Trans. Robot.*, vol. 28, no. 2, pp. 522–529, Apr. 2012, https://doi.org/10.1109/TRO.2011.2172699.

[24] M. Bryson and S. Sukkarieh, "Observability analysis and active control for airborne SLAM," *IEEE Trans. Aerosp. Electron. Syst.*, vol. 44, no. 1, pp. 261–280, Jan. 2008, https://doi.org/10.1109/TAES.2008.4517003

[25] C. Leung, S. Huang, and G. Dissanayake, "Active SLAM using model predictive control and attractor-based exploration," *IEEE Int. Conf. Intell. Robot. Syst.*, pp. 5026–5031, 2006, https://doi.org/10.1109/IROS.2006.282530.

[26] R. Hermann and A. J. Krener, "Nonlinear Controllability and Observability," *IEEE Trans. Automat. Contr.*, vol. 22, no. 5, pp. 728–740, 1977, https://doi.org/10.1109/TAC.1977.1101601.

[27] Y. Liang, L. Han, X. Dong, Q. Li, and Z. Ren, "A quantitative method for observability analysis and its application in SINS calibration," *Aerosp. Sci. Technol.*, vol. 103, p. 105881, Aug. 2020, https://doi.org/10.1016/j.ast.2020.105881.

[28] Z. Hu, T. Chen, Q. Ge, and H. Wang, "Observable degree analysis for multi-sensor fusion system," *Sensors (Switzerland)*, vol. 18, no. 12, 2018, https://doi.org/10.3390/s18124197.

[29] F. M. Ham and R. Grover Brown, "Observability, Eigenvalues, and Kalman Filtering," *IEEE Trans. Aerosp. Electron. Syst.*, vol. AES-19, no. 2, pp. 269–273, 1983, https://doi.org/ 10.1109/TAES.1983.309446.

[30] R. Sharma, "Observability-based control for cooperative localization," *2014 Int. Conf. Unmanned Aircr. Syst. ICUAS 2014 - Conf. Proc.*, pp. 134–139, 2014, https://doi.org/10.1109/ICUAS.2014.6842248.

[31] V. Lystianingrum, B. Hredzak, V. G. Agelidis, and V. S. Djanali, "Observability degree criteria evaluation for temperature observability in a battery string towards optimal thermal sensors placement," 2014, https://doi.og//10.1109/ISSNIP.2014.6827641

[32] F. W. J. Van Den Berg, H. C. J. Hoefsloot, H. F. M. Boelens, and A. K. Smilde, "Selection of optimal sensor position in a tubular reactor using robust degree of observability criteria," *Chem. Eng. Sci.*, vol. 55, no. 4, pp. 827–837, Feb. 2000, https://doi.org/10.1016/S0009-2509(99)00360-7. https://doi.org/10.1016/S0009-2509(99)00360-7.

[33] P. Batista, C. Silvestre, and P. Oliveira, "Single range aided navigation and source localization: Observability and filter design," *Syst. Control Lett.*, vol. 60, no. 8, pp. 665–673, 2011, https://doi.org/10.1016/j.sysconle.2011.05.00.

[34] P. Zhuo, Q. Ge, T. Shao, Y. Wang, and L. Bai, "Observable degree analysis using unscented information filter for nonlinear estimation systems," *2015 10th Int. Conf. Information, Commun. Signal Process. ICICS 2015*, 2016, https://doi.org/10.1109/ICICS.2015.7459932.

[35] Y. Han, C. Wei, R. Li, J. Wang, and H. Yu, "A novel cooperative localization method based on IMU and UWB," *Sensors (Switzerland)*, vol. 20, no. 2, 2020, https://doi.org/10.3390/s20020467.

[36] W. Xu, D. He, Y. Cai, and F. Zhang, "Robots' State Estimation and Observability Analysis Based on Statistical Motion Models," *IEEE Trans. Control Syst. Technol.*, vol. 30, no. 5, pp. 2030–2045, Oct. 2022, https://doi.og/10.1109/TCST.2021.3133080.

[37] K. W. Lee, W. S. Wijesoma, and I. G. Javier, "On the observability and observability analysis of SLAM," *IEEE Int. Conf. Intell. Robot. Syst.*, pp. 3569–3574, 2006, https://doi.org/10.1109/IROS.2006.281646.

[38] J. A. Hesch, D. G. Kottas, S. L. Bowman, and S. I. Roumeliotis, "Camera-IMU-based localization: Observability analysis and consistency improvement," Int. J. Rob. Res., vol. 33, no. 1, pp. 182–201, Nov. 2014, https://doi.org/10.1177/0278364913509675.

[39] S. Elahian, M. A. Amiri Atashgah, and B. Tarverdizadeh, "Collaborative Autonomous Navigation of Quadrotors in Unknown Outdoor Environments: An Active Visual SLAM Approach," *IEEE Access,* 2024, https://doi.org/10.1109/ACCESS.2024.3473792.

[40] T. Dam, G. Chalvatzaki, J. Peters, and J. Pajarinen, "Monte-Carlo Robot Path Planning," *IEEE Robot. Autom. Lett.*, vol. 7, no. 4, pp. 11213–11220, Oct. 2022,

https://doi.org/10.1109/LRA.2022.3199674.
[41] H. Mwenegoha, T. Moore, J. Pinchin, and M. Jabbal, "Model-based autonomous navigation with moment of inertia estimation for unmanned aerial vehicles," S*ensors (Switzerland)*, vol. 19, no. 11, Jun. 2019, https://doi.org/10.3390/s19112467.
[42] Y. Yang and G. Huang, "Aided Inertial Navigation with Geometric Features: Observability Analysis," *in Proceedings - IEEE International Conference on Robotics and Automation*, Sep. 2018, pp. 2334–2340, https://doi.org/10.1109/ICRA.2018.8460670.
[43] J. Kim, … S. S. R. and A. (Cat. N., and undefined 2003, "Airborne simultaneous localisation and map building," *2003 IEEE International Conference on Robotics and Automation (Cat. No.03CH37422)* 2003. https://doi.org/10.1109/ROBOT.2003.1241629.
[44] M. W. M. Gamini Dissanayake, P. Newman, S. Clark, H. F. Durrant-Whyte, and M. Csorba, "A solution to the simultaneous localization and map building (SLAM) problem," I*EEE Trans. Robot. Autom*., vol. 17, no. 3, pp. 229–241, Jun. 2001, https://doi.org/10.1109/70.938381.
[45] S. Huang, N. M. Kwok, G. Dissanayake, Q. P. Ha, and G. Fang, "Multi-step look-ahead trajectory planning in SLAM: Possibility and necessity," *Proc. - IEEE Int. Conf. Robot. Autom.,* vol. 2005, pp. 1091–1096, 2005, https://doi.org/10.1109/ROBOT.2005.1570261.
[46] M. Serpas, G. Hackebeil, C. Laird, and J. Hahn, "Sensor location for nonlinear dynamic systems via observability analysis and MAX-DET optimization," *Comput. Chem. Eng.,* vol. 48, pp. 105–112, 2013, https://doi.org/10.1016/j.compchemeng.2012.07.014.
[47] A. Nemra and N. Aouf, "Robust airborne 3D visual simultaneous localization and mapping with observability and consistency analysis," *J. Intell. Robot. Syst. Theory Appl.*, vol. 55, no. 4–5, pp. 345–376, Aug. 2009, https://doi.org/10.1007/s10846-008-9306-6.
[48] R. Aguilar-López, J. Mata-Machuca, and R. Martinez-Guerra, "On the observability for a class of nonlinear (Bio)chemical systems," *Int. J. Chem. React. Eng*., vol. 8, 2010, https://doi.org/10.2202/1542-6580.2052.
[49] N. Powel and K. A. Morgansen, "Empirical Observability Gramian for Stochastic Observability of Nonlinear Systems," 2020. Accessed: Dec. 24, 2020. http://doi.org/10.48550/arXiv.2006.07451.
[50] L. Huang, J. Song, and C. Zhang, "Observability analysis and filter design for a vision inertial absolute navigation system for UAV using landmarks," *Optik (Stuttg),* vol. 149, pp. 455–468, 2017, https://doi.org/10.1016/j.ijleo.2017.09.060.
[51] D. Goshen-Meskin and I. Y. Bar-Itzhack, "Observability Analysis of Piecewise Constant Systems Part I: Theory," *IEEE Trans. Aerosp. Electron. Syst.*, vol. 28, no. 4, pp. 1056–1067, 1992, https://doi.og/10.1109/7.165367.
[52] S. Brunton and J. Kutz, Data-driven science and engineering: Machine learning, dynamical systems, and control. 2022, https://doi.org/10.1017/9781108380690.
[53] M. H. Kazma and A. F. Taha, "Observability for Nonlinear Systems: Connecting Variational Dynamics, Lyapunov Exponents, and Empirical Gramians," Feb. 2024, Accessed: Dec. 20, 2024. [Online]. Available: http://arxiv.org/abs/2402.14711.
[54] T. Tao, Y. Huang, F. Sun, and T. Wang, "Motion planning for SLAM based on frontier exploration," *Proc. 2007 IEEE Int. Conf. Mechatronics Autom. ICMA 2007*, pp. 2120–2125, 2007, https://doi.org/10.1109/ICMA.2007.4303879.
[55] C. Yang, L. Kaplan, and E. Blasch, "Performance measures of covariance and information matrices in resource management for target state estimation," IEEE Trans. Aerosp. Electron. Syst., vol. 48, no. 3, pp. 2594–2613, 2012, https://doi.org/10.1109/TAES.2012.6237611.

HOW TO CITE THIS ATRICLE

M.-A. Amiri Atashgah, S. Elahian, and B. Tarvirdizadeh, "Observability-Guided Autonomous Path Planning for Quadrotor Navigation in GNSS-Denied Environments," *Journal of Aerospace Science and Technology,* Vol. 18, Issue 2, 2025, pp. 25-34.

DOI: https://doi.org/10.22034/jast.2025.470258.1201

URL:https://jast.ias.ir/article_218675.html